

A Modified SVPWM technique for PMBLDC Motor for DC-link current control

Indira Damarla^{1*}, Venmathi Mahendran², V. Krishnakumar³, P. Anbarasan⁴

¹Assistant Professor, Electrical and Electronics Engineering, Velagapudi Ramakrishna Siddhartha Engineering College, Siddhartha Academy of Higher Education Deemed to be University, Vijayawada, India, +91-9160620632, Email: indira@vrsiddhartha.ac.in

²Associate Professor, Electrical and Electronics Engineering, St.Joseph's College of Engineering, OMR, Chennai, India, +91-9841978226, Email: venmathim@stjosephs.ac.in

³Associate Professor, Electrical and Electronics Engineering, St.Joseph's College of Engineering, OMR, Chennai, India, +91-9944235136, Email: v_krishnakumar@ymail.com

⁴Associate Professor, Electrical and Electronics Engineering, St.Joseph's Institute of Technology, OMR, Chennai, India, +91-9176019772, Email: p.anbarasan@gmail.com

Abstract:

The permanent magnet brushless DC (PMBLDC) motor has proven enhanced performance over new classes of motors. The vector-controlled PMBLDC motor is mainly required for speed control drives such as electrical vehicles, robotics, and automotive industries. These motor drive systems typically incorporate a DC-link capacitor and position sensors. In PMBLDC motors, torque is significantly affected by the commutation pattern and phase current. The commutation process involves using the DC-link capacitor to reverse the current direction, resulting in considerable fluctuations in the torque profile. However, the conventional space vector pulse width modulation (SVPWM) technique falls short in effectively minimizing torque ripple, especially in automotive applications. To address this challenge, a modified field-oriented control (FOC) based SVPWM technique is proposed. This method prevents the reversal of DC-link current, thereby reducing torque ripple during commutation. The various operating modes of the proposed technique are comprehensively explained. By eliminating DC-link current reversal, the FOC-based SVPWM technique achieves a notable reduction in torque ripple. The proposed approach has been validated through simulations conducted using the Matlab Simulink toolbox, and experimental results obtained using an FPGA controller further confirm the effectiveness of the simulation findings.

Keywords: PMBLDC motor drive, Current control, DC-link, SVPWM, Torque ripple.

1. Introduction

A smart, energy-efficient lifestyle has emerged as a key development factor for enhanced drives in modern technology. This leads to the development of PMBLDC motor with the special features like reliability, simple maintenance, higher torque-volume proportion,

empowered mechanical and electrical benefits and superior torque. These features make it to be used in various applications like medical equipment, electric vehicle, elevators, and robotic machine tools etc., Both the permanent magnet AC and DC motors, uses the voltage source inverter as drive circuit for its basic actuation [1-3].

Dynamic execution has been carried out during normal operation of the field-oriented control. But BLDC produces high torque ripple during phase commutation sequence irrespective of its special features. This is because of the inductive nature of stator coil, when any one of the phases being commutated, then the resultant shapes of current and back EMF are turned off from its original wave shapes and hence motor contributes to torque pulsations. Hence it becomes necessary to control the torque ripple which in turn controls the position and the speed. Otherwise, it leads vibration and acoustic noise [4-8]. A modified hybrid switching selection mode has been investigated for minimizing the torque ripple. Hybrid inverter phase selection either two or three phase switching engaged in the commutation duration has also been developed [9]. Torque pulsations mitigation has been achieved by incorporating certain nonlinear equations derived in addition with vector-controlled strategy for BLDCM drive [10-11]. Sensor-less torque control and flux control have been applied to permanent magnet motors, where direct torque control is preferred; however, this is only applicable to medium speed drive applications. Sensor-less control of BLDC motors is becoming mandatory in hazardous environments [12]. The control of stator flux linkage has been demonstrated along with its possibility even without PI controllers. It is difficult to ensure constant reference of stator flux, as the flux of rotor is not sinusoidal in nature, hence Implementation of dc-dc conversion systems has been discussed for BLDCM drive circuit to improve the torque quality [13].

The inverter with four switch drive has been suggested for BLDCM, where the control signals are effectively generated based on voltage vector look up table. Based on the switching instants the optimal torque has been controlled [14]. Aside from the changes in topology, retraction of torque ripple has been endeavored through certain PWM strategy modification. A direct torque control-based hybrid SVPWM has been attempted to induction motor drive in which imaginary switching times has been framed to minimize the steady state current ripple [15]. The switching instant has been computed from the voltage signals. This could be the comparative difference between the estimated and reference flux vectors. The stator flux ripple control has been the primary idea, since it has been directly linked with the line current ripple. To limit the commutated ripple torque, an integration of simple square wave with PWM strategy has been developed along with the signals of position sensor [16]. A novel Current limit approach to restrain the rise in voltage of DC link capacitor for BLDCM has been

developed. The current limit strategy employs half-turn OFF logic of switches instead of all-switches turned OFF logic of inverter. The suggested current limit approach eliminates the current reversion [17]. The Direct torque control (DTC) approach for BLDC motor drive has been developed to reduce torque ripple during sector-to-sector commutation [18]. The vector selection table for three different approaches has been developed and attempted to sort the best optimal DTC strategy among the three to accomplish reduced torque ripple [19-20]. A novel Direct Torque controller has been recommended for BLDCM to minimize the torque ripple. This uses three-level torque controllers instead of two-level controller which enables to improve the drive reliability. This strategy balances the average switching frequencies in both upper and lower switches, reduces the common mode voltage, attenuates the torque ripple amplitude using vector selection table [21].

The direct power control (DPC) approach has been designed and implemented for brushless DC generator which uses minimum controller and sensors. A novel Adaptive nonlinear internal model speed controller has been discussed for homopolar BLDCM. The suggested speed control block utilizes negative feedback speed difference of motor and its nonlinear internal model output, to subdue the reference speed error. The controller signal has been synthesized to the inverter power switches to unite the motor speed with intended speed [22-24]. The novel power converter topology has been implemented to BLDCM to dispense the torque ripple during phase current commutation. Novel commutation optimization topology has also been recommended to BLDC motor. The proposed topology has the ability to avoid the inaccuracies in commutation position caused by installation errors of hall sensors [25-26]. The design of novel combined two and three legs conducting controlling has been discussed based on the overlap angle control. The attractive option overlap angle features to minimize the torque ripple and winding losses. Phase locked loop (PLL) controller-based BLDC motor has been suggested to investigate the non-ideal factors which reduces the commutation error to zero [27-28]. The phase current regulation technique to minimize the torque ripple has been suggested for single phase BLDCM for turbocharger application [29]. The studies from the published works indicate that many analysts are interested in improving the torque performance of PMBLDCM drives.

This work emphasizes on the reversal of torque ripple in PMBLDC motors under commutation. The controller has been implemented for the phase current in addition to the regulated process of commutation and the inversion of dc-link current. The proposed FOC-PMBLDCM has been simulated using MATLAB/Simulink tool. The system has also provided satisfactory experimental results.

2. Mathematical Modeling of PMBLDC Motor

The PM Brushless DC Motor consists of three-phase stator windings, each spaced 120 degrees apart, and a permanent magnet rotor. These stator windings are energized to produce a back EMF. The permanent magnet rotor commonly utilizes samarium cobalt due to its good magnetic properties compared to other rare earth magnets. The magnet on the rotor needs to have a higher magnetic density to enable a smaller rotor size, achieve an optimal size-to-weight ratio, and deliver greater torque. It's crucial to maintain nearly uniform flux density across the air gap between the permanent magnet rotor and the stator winding. Estimation of the rotor position is essential for BLDCM control, and it achieved through Hall Effect sensors. The appropriate commutation sequence is determined by sensor signals. Due to non-linearities in the commutation process, only two phases are excited with current at any given instant, resulting in a significant torque ripple. Figure 1 illustrates a basic control perspective of the PMBLDC motor.

The motor is considered a 3-phase star-connected stator circuit. Using flux linkage, it becomes essential to model the PM brushless machine using state variables. The self and mutual inductances of the three phases are equal when the rotor is smooth and cylindrical, and the rotor inductance angle remains constant. The stator currents i_a , i_b , and i_c are maintained as balanced, and the corresponding stator phase voltages are given in Eq. (1) to Eq. (3):

$$v_a = i_a R + (L - M) \frac{di_a}{dt} + E_a \quad (1)$$

$$v_b = i_b R + (L - M) \frac{di_b}{dt} + E_b \quad (2)$$

$$v_c = i_c R + (L - M) \frac{di_c}{dt} + E_c \quad (3)$$

E_a , E_b , and E_c are the induced back EMF for three phases, R , L , and M denotes the resistance, self and mutual inductance of the stator winding respectively. The matrix model of the stator voltages can be expressed as Eq. (4)

$$\begin{pmatrix} v_a \\ v_b \\ v_c \end{pmatrix} = R \begin{pmatrix} 1 & 0 & 0 \\ 0 & 1 & 0 \\ 0 & 0 & 1 \end{pmatrix} \begin{pmatrix} i_a \\ i_b \\ i_c \end{pmatrix} + (L - M) \begin{pmatrix} 1 & 0 & 0 \\ 0 & 1 & 0 \\ 0 & 0 & 1 \end{pmatrix} \frac{d}{dt} \begin{pmatrix} i_a \\ i_b \\ i_c \end{pmatrix} + \begin{pmatrix} E_a \\ E_b \\ E_c \end{pmatrix} \quad (4)$$

The generated torque and speed can be computed from Eq. (5) and Eq. (6)

$$T_g = \frac{E_a i_a + E_b i_b + E_c i_c}{\omega} \quad (5)$$

$$E = f(\theta_r)\psi\omega \quad (6)$$

where θ_r is the rotor position, ψ is the flux linkage, and ω is the angular velocity. Hence, the developed rotor torque can be given in Eq. (7)

$$T_g = \psi[f_a(\theta_r)i_a + f_b(\theta_r)i_b + f_c(\theta_r)i_c] \quad (7)$$

The expression for an angular velocity with respect to inertia constant J and frictional coefficient B with torque T_L can be represented as Eq. (8) and Eq. (9)

$$\omega = \frac{1}{J} \int (T_g - T_L - B\omega) dt \quad (8)$$

$$\frac{d\theta}{dt} = \frac{P}{2} \omega \quad (9)$$

3. Cause of Reversal of DC link current

The performance analysis of the BLDCM drive during speed changes, startup, and load variations is a key focus in design considerations. Initially, the transition of phases may involve commutation between upper arm switches. Later, their corresponding diode circulates the current, resulting in current polarity inversion. Similarly, it also exists between the two lower arm diodes D_4 and D_6 during the commutation. This commutation intervals causes the reversal of DC-link current (I_{dc}), leading to increased torque ripple, as shown in Figure 2. Such disturbances can harm capacitors connected to the DC voltage source. The DC-link current limiter is essential for protection.

The point X in Figure 2 is regarded as a load change point since it causes the motor phase current to increase over the threshold. Under normal conduction instant, the phase current enters the DC-link. However, during the phase transition, the DC-link current rushes, causing the DC-link current to circulate in the opposite direction, which causes a fast spike in the capacitor voltage. Even with the all switches pulsed OFF technique, this condition cannot be altered. When the detected current in the dc-link exceeds its threshold value, S_1 is ON and S_2 is OFF. Similarly, the switch S_2 , D_4 , and D_6 cause the S_2 to turn ON and the S_1 to turn OFF, directing the phase current circulation to the lower leg of VSI.

4. Proposed FOC based SVPWM controlled BLDCM drive System

This proposed topology's primary objective is to control the current using vector control. The proposed FOC based SVPWM technique for BLDC motor drive system is shown in Figure 3. Using Clark transformation, the current and back EMF signals of the three-phase components can be converted into two-phase components E_{dq} and I_{dq} . The speed, rotor position θ , torque, and rotor flux linkage are determined using an electrical parameter estimator. The

controller calculates the reference torque based on the error. The i_d component is maintained at zero, and torque control is achieved through the i_q component. The θ value is detected and a signal is sent to the SVPWM technique. The derived equations are presented Eq. (10) to Eq. (12).

$$i_{ds}^* = \frac{V_d}{L} - \frac{R}{L}i_{ds} + \omega * i_{qs} \quad (10)$$

$$i_{qs}^* = \frac{V_q}{L} - i_{qs} \frac{R}{L} - \frac{\varphi}{L} \omega - \omega * i_{ds} \quad (11)$$

$$\omega = i_d i_{qs}^* - i_q i_{ds}^* - (i_{qs}^* - i_{ds}^*) \frac{\varphi}{L} \quad (12)$$

The aforementioned FOC-integrated SVPWM-controlled BLDCM features the enhancements in performance that do not compromise its basic functionality being highly desirable.

4.1 FOC based SVPWM Switching pattern for DC link Current Control Strategy

The conventional SVPWM scheme for BLDC motors involves switch turn-off using zero vectors, either digitally represented as (0,0,0) or (1,1,1). During the active period, the phase current aligns with the DC-link current, which leads to a decrease in torque ripple when the active vector switching is chosen. According to fundamental SVM theory, after completing the conduction period with non-zero vectors, zero switching logic vectors are introduced to ensure commutation. Throughout this transition, the positive pole of the DC-link is reconnected through to the negative pole through diode, as the next phase switches from the negative to the positive pole. This polarity inversion can cause a reversal of the DC-link current.

PWM current control algorithm is typically preferred for BLDCM because of its linear relationship between torque and phase current. To meet the electromagnetic torque requirements and prevent the reversal of DC-link current during phase transitions, an enhanced SVM scheme is introduced. This scheme ensures an Enforced Single Switch Turn-On (ESSTO) position during commutation, preventing phase current reversal in either the positive or negative DC rail. This is based on a comparison between the threshold current (I_{th}) and the actual current (I_{dc}). The Pseudo Dead Time SVPWM technique ensures a unidirectional flow of current by enforcing a single switch dead time. Tables 1 illustrate the switching pattern for the proposed SVPWM scheme for a complete operational cycle.

Figure 4 shows the developed SVM switching pattern diagram for the DC-link control strategy. Six voltage vectors are actively used to generate the switching sequence for a three-phase inverter. The six active voltage vectors, denoted by V_{L1} , V_{L2} , V_{L3} , V_{L4} , V_{L5} , and V_{L6} produce digital pulses for the conduction modes in the three-phase inverter, along with the

zero-voltage vector represented by V_0 . The switching combinations of $S_1, S_2, S_3, S_4, S_5, S_6$ correspond to the six active voltage vectors V_{L1} to V_{L6} depicted in the α - β plane: $V_{L1}(110000)$, $V_{L2}(011000)$, $V_{L3}(001100)$, $V_{L4}(000110)$, $V_{L5}(000011)$, and $V_{L6}(100001)$ for phases a, b, and c.

4.2 Analysis of Proposed Topology:

Case 1: Regular Conduction mode ($I_{dc} < I_{th}$)

In this case, the DC link current is below threshold so the active voltage vector matches the hall signal chosen by the segment selector. Hence, during the modes 1-6 in which the corresponding time interval is t_1 - t_6 , therefore inverter works in conduction period.

Case 2: Proposed Turned ON/Turned OFF method ($I_{dc} > I_{th}$)

During the commutation interval, the segment selector turns ON the proposed enforced single switch rather than inserting the zero vector. Figure 5(a) and Figure 5(b) shows the operation of this mode, in which the Enforced Single switch turn on instead of turning all switches OFF using zero vector V_0 . In order to restore the switching action, this continuously sends a signal to the sampling block ensuring that I_{dc} remains within the I_{th} , as shown in Table 1. As shown in Figure 6, the promotion of uncontrolled commutation process of traditional SVPWM is introduced when the current has arrived a steady value relates to the varying new load. Therefore, a new sampling strategy is proposed to ascertain the right time to turn off the switching based on the DC link current.

Figure 7(a) shows the switching waveforms under conduction and commutation intervals. The dc-link's current is limited by the selector logic, which allows the signal from driver circuit to power switch S_2 next to the switch S_1 until the followed sampling cycle when $I_{dc} < I_{th}$. If $I_{dc} > I_{th}$, then it enables the stop pulse to turned off the switch S_2 . Figure 7(b) clarifies the sampling of switching for both turned ON and OFF position of switch S_2 . Under regular working (t_1 - t_2), the dc-link current is typically sampled with derived frequency. When current increases at instant t_2 , the control signal is turned OFF, the switch S_2 is turned OFF. After this enable logic selection signal enables the re-sample signal at t_3 and confines the applicable current limit within the interval of samplings.

5. Simulation Results & Discussions

Table 2 contains a list of the simulation parameters. The simulation results confirm the viability of the current limit method for BLDCM drive using the FOC technique. The

performance is analyzed using MatLab simulink tool for the fully turned off condition and single switch turned off condition.

5.1 Steady state analysis and validation

The PMBLDC motor's performance has been verified through a steady state analysis using both conventional and proposed techniques.

Case 1: Conventional SVPWM Commutation technique

At start, the performance of PMBLDC motor is investigated based on conventional SVPWM technique. In this approach, all the switches are turned OFF during the commutation process. Figure 8(a) and Figure 8(b) represents simulated results of motor dc-link current and phase currents respectively. It is to be observed that, dc-link current varies between -8A to 8A because of the inversion of dc-link voltage. In Figure 9, the voltage of dc-link capacitor boosts up to 245V, which may cause significant issue on dc-link capacitor and torque of the motor.

Case 2: Proposed FOC based SVPWM Commutation technique

In proposed commutation technique, only one switch operated to prevent the negative portion of DC-link current. During this point, there occurs a commutation period between the inverter switches and the motor winding, which is represented at Figure 10. The corresponding phase current and the dc link current of the motor are shown in Figures 11 and 12. Figure 12 has a flat top shape, which is significantly smaller when all the switches are turned OFF technique.

5.2 Transient analysis and its validation

The transient state analysis has been carried out to validate the performance of PMBLDC motor with the conventional and proposed techniques.

Case 1: Conventional SVPWM Commutation technique

Figure 13 displays the motor's transient characterization performance using standard SVPWM. Under the transient performance test, the motor changed from maintaining 12Nm at 0.25ms to 9Nm. It is very clearly demonstrated the dc-link current reversal from Figure 13, at 0.5ms the speed of motor is drop down towards zero (stop signal), however the capacitor makes reversal circulation of current. Henceforth, because of the reversal of the dc-link current, increase in voltage is 100V to 230V nearly 130% higher voltage than normal, which may decrease the life span of dc-link capacitor.

Case 2: Proposed FOC based SVPWM Commutation Technique

The investigation of proposed commutation method with similar parameters has been considered and the results are presented in Figure 12. At 100V V_{dc} , the dc-link current reaches its maximum level of assistance. Figure 14 shows that the dc-link current reversal is

significantly reduced. This is achieved by developing a commutation that prevents looping between the motor winding's back EMF energy and the dc-link capacitor, allowing for reduced torque fluctuations and longer capacitor life.

The torque fluctuation is verified by Figures 13 and 14, which support the proposed privileged turn OFF methodology. For both the proposed and conventional topologies, the torque ripple has been calculated and is reported as 36.36% and 8.82%, respectively. Therefore, compared to the conventional technique, the proposed control technique lowers the torque ripple in the PMBLDC motor.

6. Experimental Validation

A hardware implementation is developed to authenticate the results obtained from simulation of the developed BLDCM drive. The real time implementation is depicted in Figure 15. The microelectronics STGD18N40LZT4–ST based intellectual power module (IPM) with capacity of link capacitor 100 μ F is utilized. The dc-link voltage is considered as 100V. The BLDC motor specified parameters are listed in Table 2.

To validate the proposed control technique, a controller board of Xilinx Spartan-III 3 AN-XC3S400 is utilized. The processing unit utilized to determine the DC link and phase current from relevant sensors.

The control signal is applied for selecting proper switching options. The look up table (LUT) has been utilized to store the regular switching patterns and commutation instants; the stored signal is used to generate the trigger pulse to drive the control logic circuit for dc-link control from processing unit. The conventional and proposed SVPWM topologies, commutation control switching logic has been stored. At first the test set up is made with conventional method. The pulses of switching for VSI have been shown in Figure 16.

In Figure 17 and 18 shows the phase currents for both the cases conventional and proposed strategies. In Figure 19 depicts the motor phase current and dc-link current. To relate the control strategies for current and torque ripple for the proposed topology, a torque response is recorded using the optical sensor linked to the motor shaft. The measured response is captured using the computer which is connected to torque sensor.

The specifications of torque sensor are 1500RPM, 5Nm. The torque waveform is seen in Figure 20(a) and Figure 20(b). From the catch results, the exploratory torque results were determined. The torque ripple of the proposed topology has been computed to 7.97% which is considerably lesser than conventional method which is 12.7%. The detailed analysis of the above torque computation validation confirms the merits of developed commutation strategy.

7. CONCLUSION

This paper presents the development of a modified SVPWM technique for a PMBLDC motor drive, aimed at evaluating its performance. The modes of operation of the proposed topology are thoroughly analysed. By preventing the dc-link current from reversing through a fully controlled commutation process, the proposed FOC-based modulation strategy reduces the torque ripple in a BLDC motor. The proposed topology performance is validated through both steady-state and transient analyses. Simulations were conducted to assess the significance of the proposed technique, with results compared to conventional modulation methods. The findings reveal that the proposed FOC-based SVPWM enhances drive performance over conventional PWM by boosting dc-link voltage, increasing average torque, and reducing torque ripple. Specifically, the proposed technique achieved a dc-link capacitor voltage twice the dc-link voltage and reduced torque ripple. The torque ripple has been calculated for both the conventional and proposed topologies and is reported as 36.36% and 8.82%, respectively. Experimental results further confirm the steady-state and dynamic behaviour of the proposed topology, aligning closely with the simulation outcomes.

REFERENCES

1. Huang, C.L., Wu, C.J., and Yang, S.C., "Full region sensorless bldc drive for permanent magnet motor using pulse amplitude modulation with dc current sensing", *IEEE Trans. Ind. Electron.*, **68**(11), pp. 11234-11244 (2021). DOI: 10.1109/TIE.2020.3034859.
2. Wang, Q., Niu, S., and Yang, L., "Design optimization and comparative study of novel dual pm excited machines", *IEEE Trans. Ind. Electron.*, **64**(12), pp. 9924-9933 (2017). DOI: 10.1109/TIE.2017.2716869.
3. Prabhu, N., Thirumalaivasan, R., and Ashok, B., "Critical review on torque ripple sources and mitigation control strategies of bldc motors in electric vehicle applications", *IEEE Access*, **11**, pp. 115699-115739 (2023). DOI: 10.1109/ACCESS.2023.3324419.
4. Wang, L., Zhu, Z.Q., Bin, H., et al. "A commutation optimization strategy for high speed brushless dc drives with voltage source inverter", *IEEE Trans. Ind. Appl.*, **58**(4), pp. 4722-4732 (2022). DOI: 10.1109/TIA.2022.3170290.
5. Jin, H., Liu, G., Li, H., et al. "A fast commutation error correction method for sensorless bldc motor considering rapidly varying rotor speed", *IEEE Trans. Ind. Electron.*, **69**(4), pp. 3938-3947 (2022). DOI: 10.1109/TIE.2021.3070493.
6. Mahmouditabar, F., Vahedi, A., and Takorabet, N., "Design and analysis of interior permanent magnet motor for electric vehicle application considering irreversible

- demagnetization", *IEEE Trans. Ind. Appl.*, **58**(1), pp. 284-293 (2022). DOI: 10.1109/TIA.2021.3126695.
7. Bosso, C., Conficoni, C., Raggini, D., et al. "A computational effective field oriented control strategy for accurate and efficient electric propulsion of unmanned aerial vehicles", *IEEE/ASME Trans. Mechatron*, **26**(3), pp. 1501-1511 (2021). DOI: 10.1109/TMECH.2020.3022379.
 8. Huang, L., Lee, F.C., Liu, C.J., et al. "Torque ripple reduction for bldc permanent magnet motor drive using dc link voltage and current modulation", *IEEE Access*, **10**, pp. 51272-51284 (2022). DOI: 10.1109/ACCESS.2022.3173325.
 9. Heidari, R., and Ahn, J.-W., "Torque ripple reduction of bldc motor with a low cost fast response direct dc link current control", *IEEE Trans. Ind. Electron*, **71**(1), pp. 150-159 (2024). DOI: 10.1109/TIE.2023.3247732.
 10. Lee, S., and Son, H., "Six steps commutation torque and dynamic characteristics of spherical brushless direct current motor", *IEEE Trans. Ind. Electron*, **71**(5), pp. 5045-5054 (2024). DOI: 10.1109/TIE.2023.3285976.
 11. Heidari, R., and Ahn, J.-W., "Torque ripple reduction of bldc motor with a low cost fast response direct dc link current control", *IEEE Trans. Ind. Electron*, **71**(1), pp. 150-159 (2024). DOI: 10.1109/TIE.2023.3247732.
 12. Masoudi, H., Kiyoumars, A., Madani, S.M., et al. "Torque ripple reduction of nonsinusoidal brushless dc motor based on super twisting sliding mode direct power control", *IEEE Trans. Transp. Electrific.*, **9**(3), pp. 3769-3779 (2023). DOI:10.1109/TTE.2023.3250950.
 13. Lee, Y., "A new method to minimize overall torque ripple in the presence of phase current shift error for three phase bldc motor drive", *Can. J. Electr. Comput. Eng.*, **42**(4), pp. 225-231 (2019). DOI: 10.1109/CJECE.2019.2907118.
 14. Li, Z., Fan, X., Kong, Q., et al. "Torque ripple suppression of bldcm with optimal duty cycle and switch state by fcs-mpc", *IEEE Open J. Power Electron.*, **5**, pp. 381-391 (2024). DOI: 10.1109/OJPEL.2024.3368221.
 15. Huang, C.L., Lee, F.C., Liu, C.J., et al. "Torque ripple reduction for bldc permanent magnet motor drive using dc link voltage and current modulation", *IEEE Access*, **10**, pp. 51272-51284 (2022). DOI: 10.1109/ACCESS.2022.3173325.
 16. Kumar, P., Bhaskar, D.V., Behera, R.K., et al. "Continuous fast terminal sliding surface based sensorless speed control of pmbldcm drive", *IEEE Trans. Ind. Electron*, **70**(10), pp. 9786-9798 (2023). DOI: 10.1109/TIE.2022.3225850.

17. Park, H., Kim, T., and Suh, Y., "Fault tolerant control methods for reduced torque ripple of multiphase bldc motor drive system under open circuit faults", *IEEE Trans. Ind. Appl.*, **58**(6), pp. 7275-7285 (2022). DOI: 10.1109/TIA.2022.3191633.
18. Zhao, D., Wang, X., Xu, L., et al. "A new phase delay free commutation method for bldc motors based on terminal voltage", *IEEE Trans. Power Electron.*, **36**(5), pp. 4971-4976 (2021). DOI: 10.1109/TPEL.2020.3039887.
19. Lee, J., Lim, G.C., and Ha, J.I., "Pulse width modulation methods for minimizing commutation torque ripples in low inductance brushless dc motor drives", *IEEE Trans. Ind. Electron.*, **70**(5), pp. 4537-4547 (2023). DOI: 10.1109/TIE.2022.3189104.
20. Wang, L., Zhu, Z.Q., Sun, X., et al. "A 12 step asynchronous pwm scheme for high speed brushless dc drives with commutation compensation", *IEEE Trans. Ind. Electron.*, **71**(10), pp. 11936-11947 (2024). DOI: 10.1109/TIE.2024.3355524.
21. Kumar, P., Beig, A.R., Bhaskar, D.V., et al. "An enhanced linear active disturbance rejection controller for high performance pmbldcm drive considering iron loss", *IEEE Trans. Power Electron.*, **36**(12), pp. 14087-14097 (2021). DOI: 10.1109/TPEL.2021.3088418.
22. Moradi, H., and Cheshmeh, B., "An adaptive nonlinear internal model control for the speed control of homopolar salient pole bldc motor", *Int. J. Electron.*, **105**(5), pp. 848-865 (2017). DOI:10.1080/00207217.2017.1409810.
23. Viswanathan, V., and Seenithangom, J., "Commutation torque ripple reduction in the bldc motor using modified sepic and three level npc inverter", *IEEE Trans. Power Electron.*, **33**(1), pp. 535-546 (2018). DOI: 10.1109/TPEL.2017.2671400.
24. Zhang, Q., and Feng, M., "Combined commutation optimization strategy for brushless dc motors with misaligned hall sensors", *Electr. Power Appl.*, **12**(3), pp. 301-307 (2017). DOI: 10.1049/iet-epa.2017.0276.
25. Chetan, K., and Rajagopalan, C.L., "Simple overlap angle control strategy for commutation torque ripple minimization in bldc motor drive", *IET Electr. Power Appl.*, **12**(6), pp. 797-807 (2018). DOI: 10.1049/iet-epa.2017.0644.
26. Gu, C., Wang, X., Shi, X., et al. "A pll based novel commutation correction strategy for a high speed brushless dc motor sensorless drive system", *IEEE Trans. Ind. Electron.*, **65**(5), pp. 3752-3762 (2018). DOI: 10.1109/TIE.2017.2760845.
27. Masoudi, H., Kiyomarsi, A., Madani, S.M., et al. "Closed loop direct power control of brushless dc motor in field weakening region", *IEEE Trans. Transp. Electrific.*, **10**(2), pp. 3482-3491 (2024). DOI: 10.1109/TTE.2023.3305050.

28. Mohanraj, D., Gopalakrishnan, J., Chokkalingam, B., et al. "Critical aspects of electric motor drive controllers and mitigation of torque ripple-review", *IEEE Access*, **10**, pp. 73635-73674 (2022). DOI: 10.1109/ACCESS.2022.3187515.
29. Sun, H., Dou, Y., and Chen, Y., "A space vector pulse width modulation method for switched reluctance motor driven by full bridge power converter", *IET Electr. Power Appl.*, **17**(11), pp. 1437-1446 (2023). DOI: <https://doi.org/10.1049/elp2.12353>.

List of Figures:

Figure 1. Structure of PMBLDC motor drive system

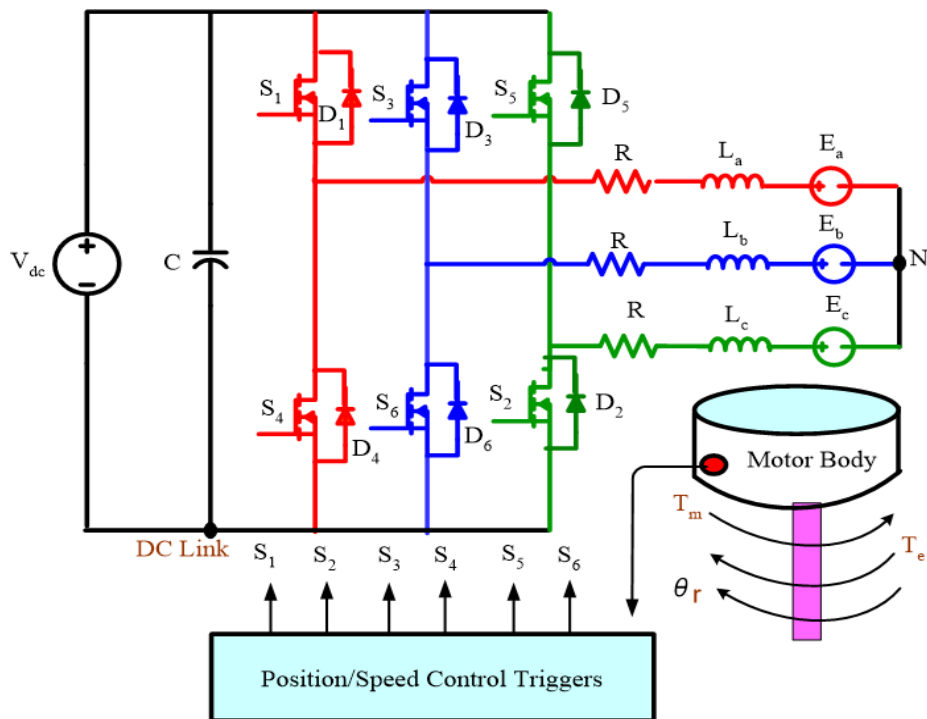


Figure 2. DC link current profile under loading conditions

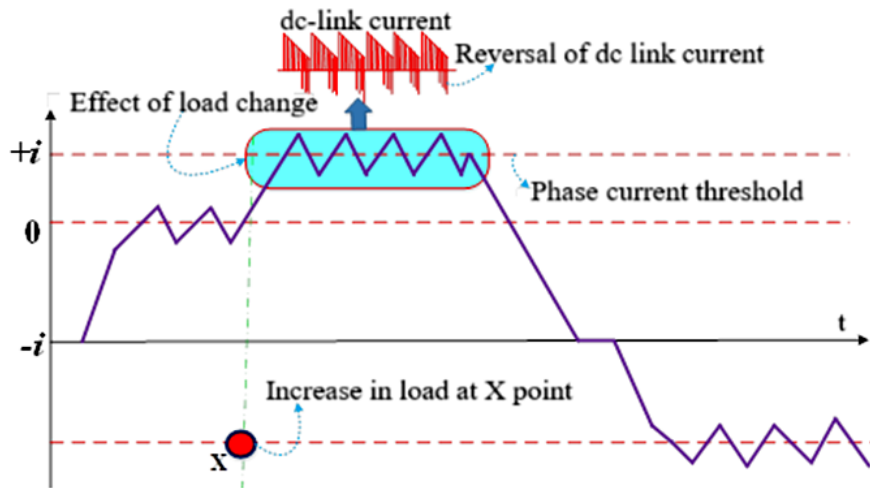


Figure 3. Block diagram representation of proposed FOC based SVPWM technique for BLDC motor drive system

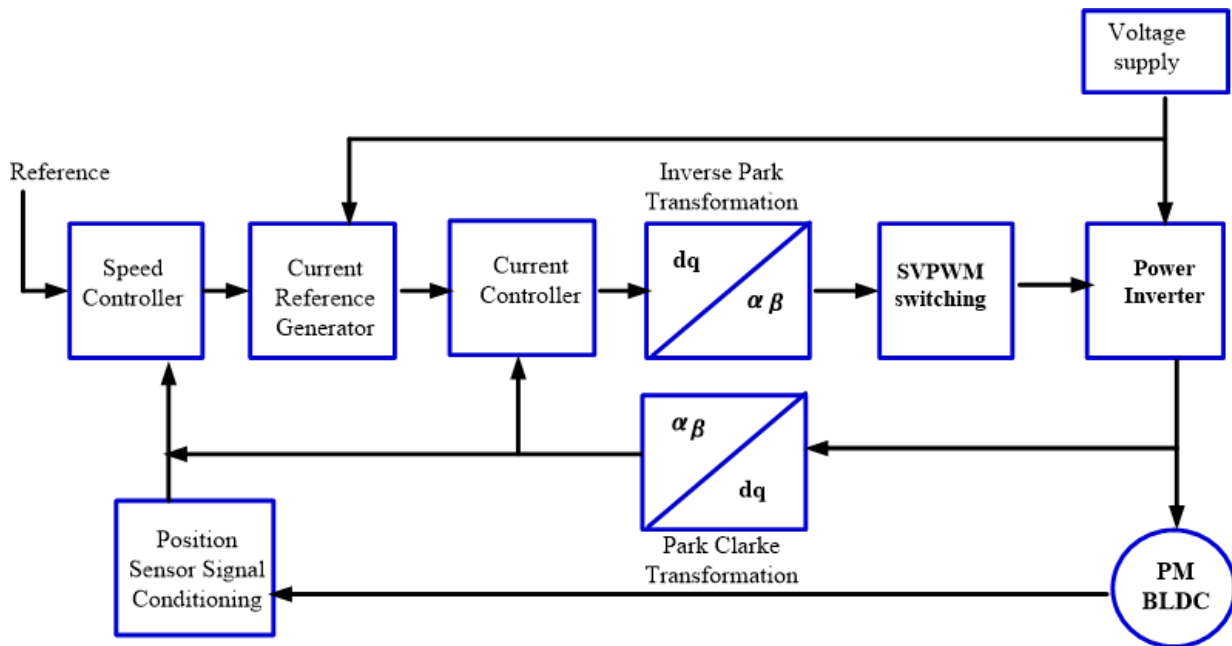


Figure 4. SVPWM Switching Pattern

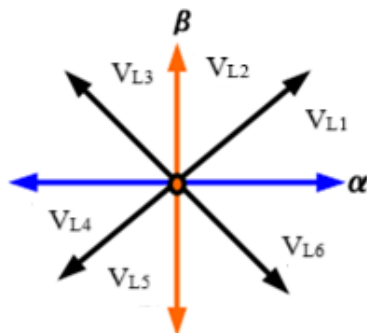


Figure 5(a). FOC-based SVPWM Commutation in upper leg

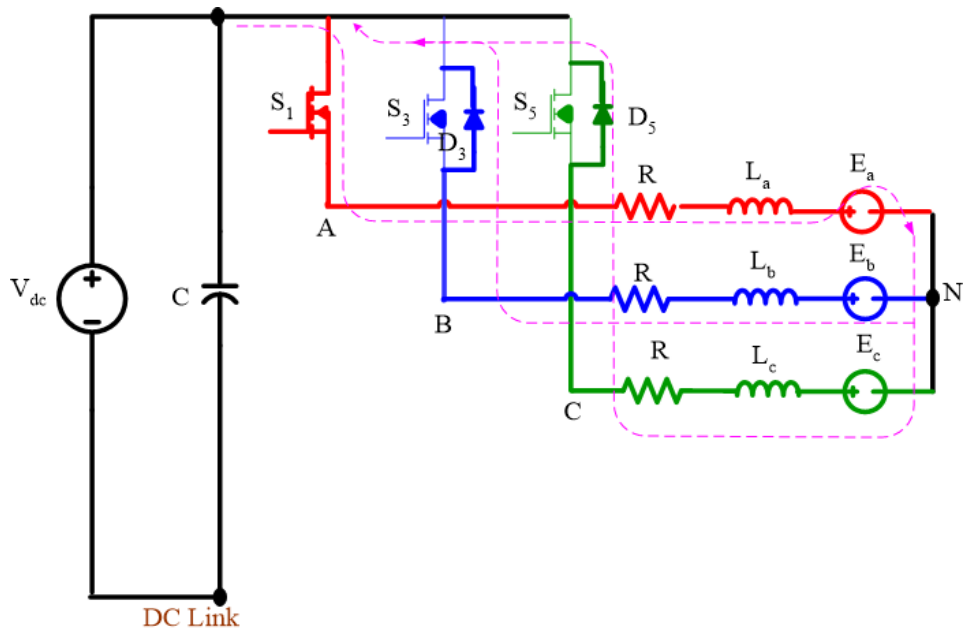


Figure 5(b). FOC based SVPWM Commutation in lower leg

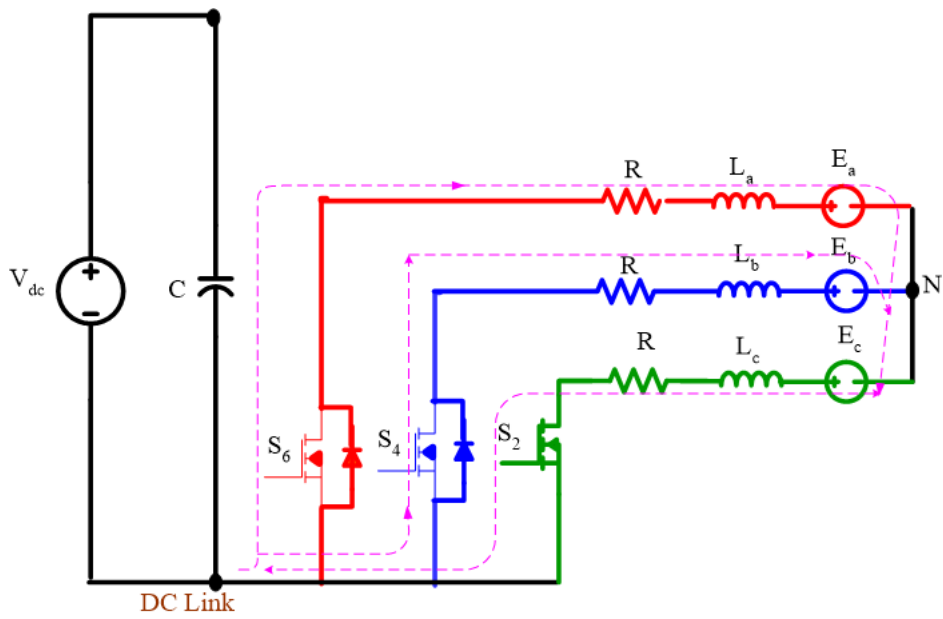


Figure. 6. PWM selection of switch during the load change

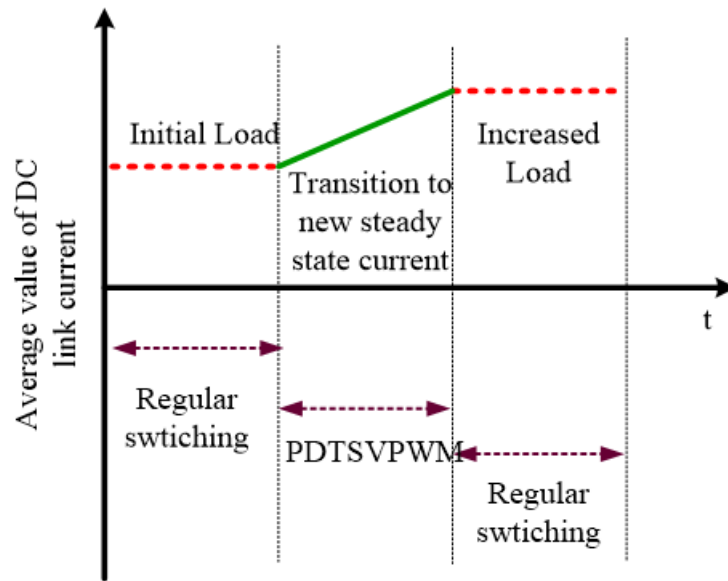


Figure 7(a). Switching waveforms

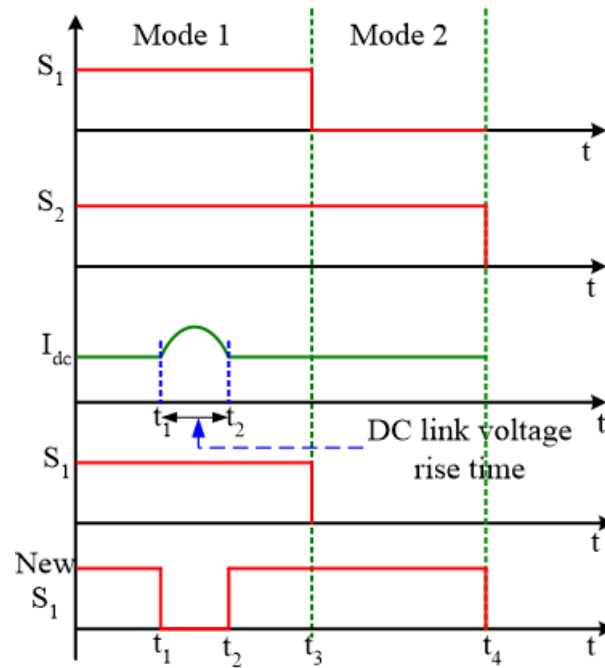


Figure 7(b). Sampling timing diagram dc-link current

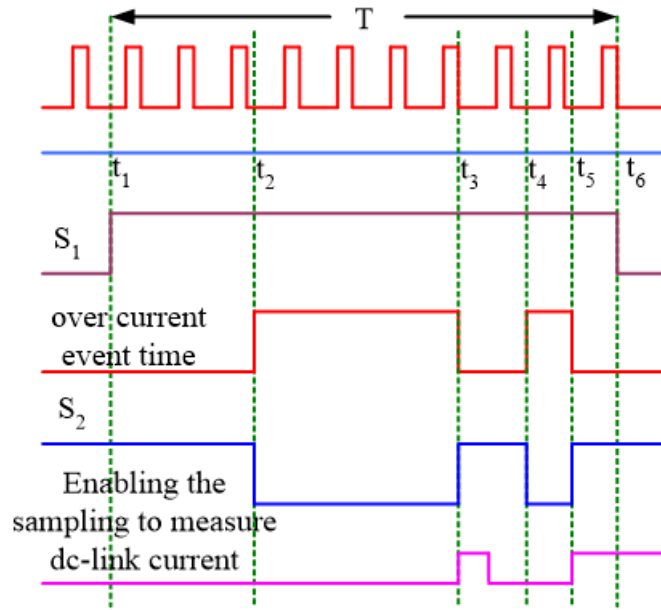


Figure 8(a). DC-link current in Conventional SVPWM topology

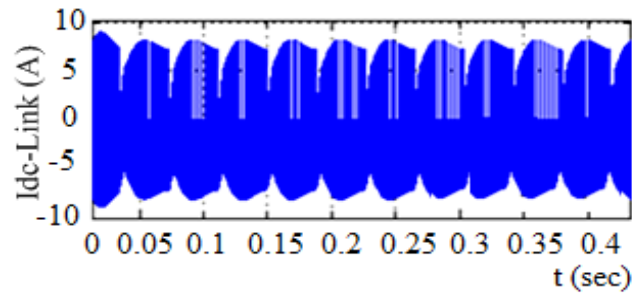


Figure 8(b). Phase current in Conventional SVPWM topology

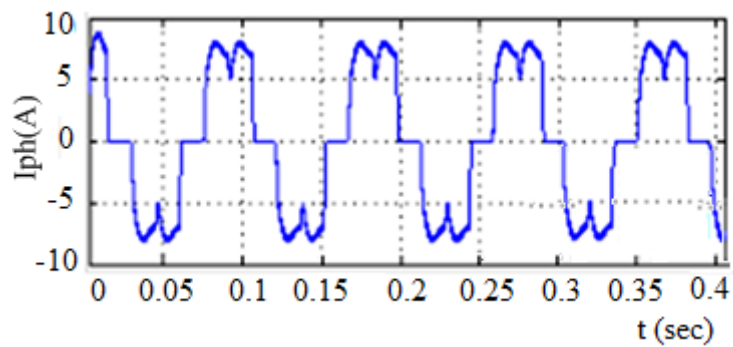


Figure 9. DC-link voltage in Conventional SVPWM topology

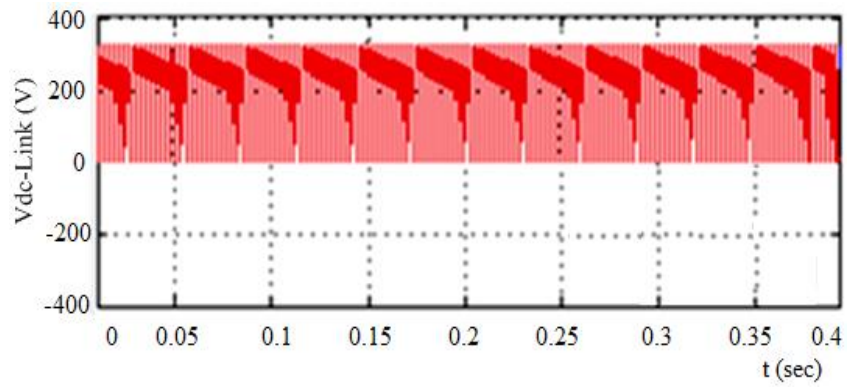


Figure 10. DC link voltage in Proposed FOC based SVPWM topology

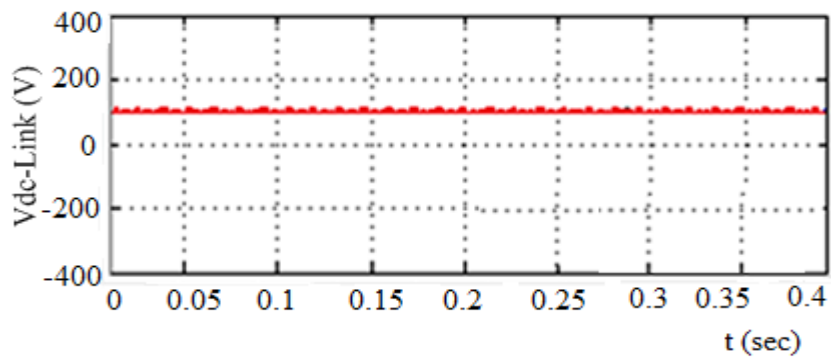


Figure 11. DC link current in Proposed FOC based SVPWM topology

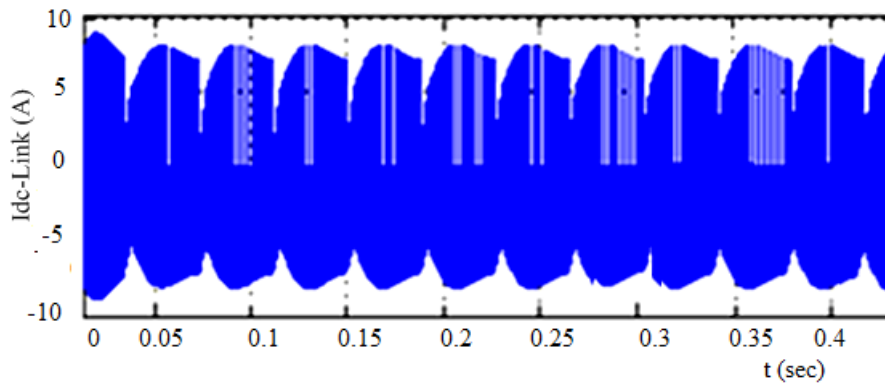


Figure 12. Phase current in Proposed FOC based SVPWM topology

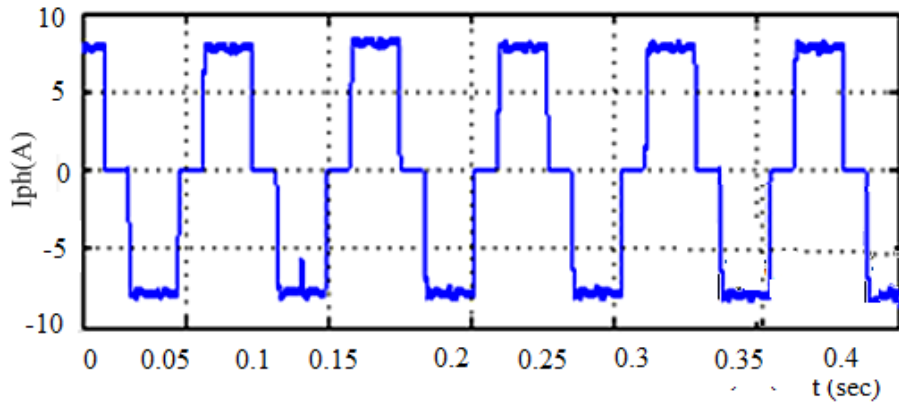


Figure 13. Transient analysis for conventional SVPWM topology

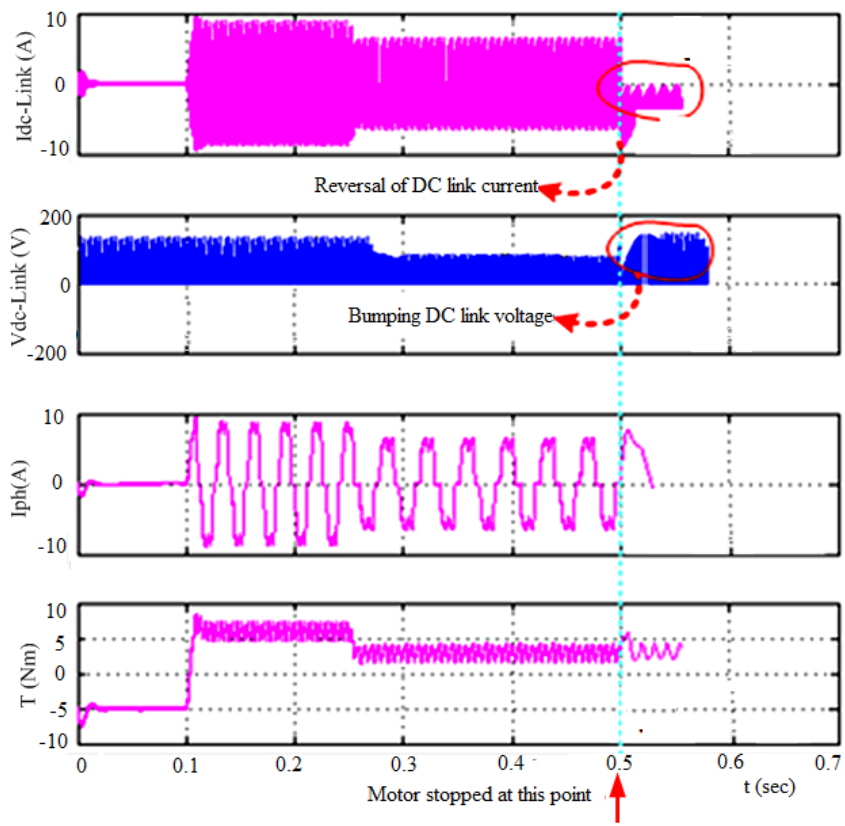


Figure 14. Transient analysis for proposed FOC based SVPWM topology

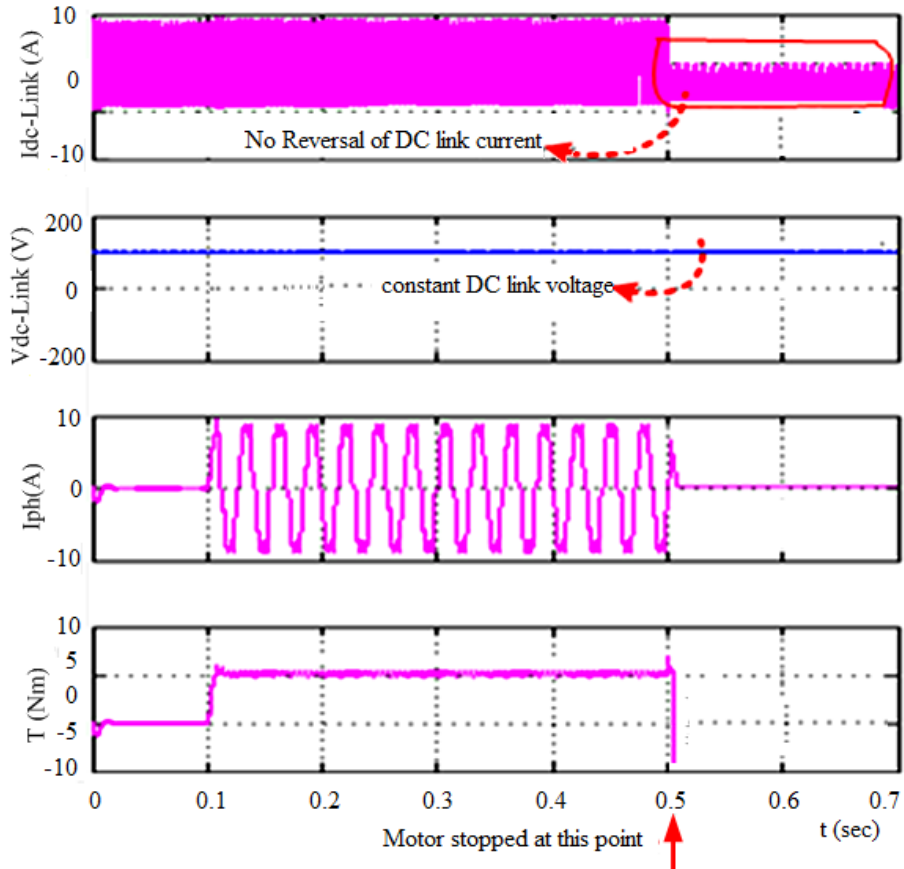


Figure 15. Hardware Prototype for PMLBDC Motor Drive System



Figure 16. Switching pulses for the proposed FOC based SVPWM topology

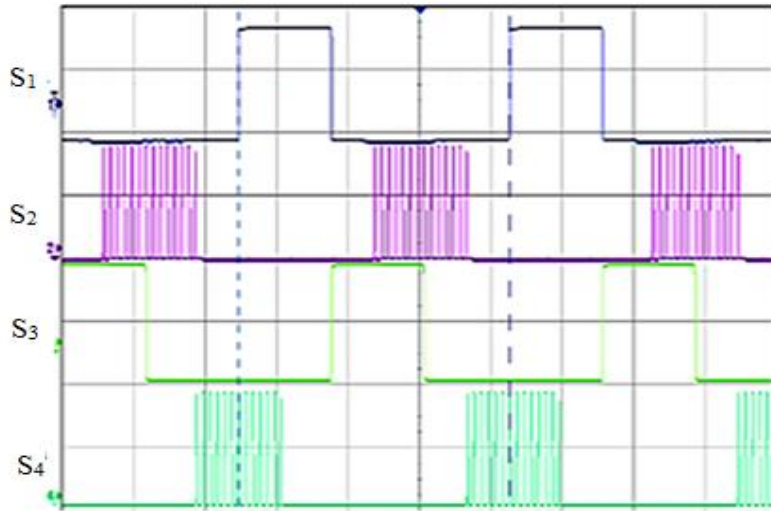


Figure 17. Phase Current in Conventional topology

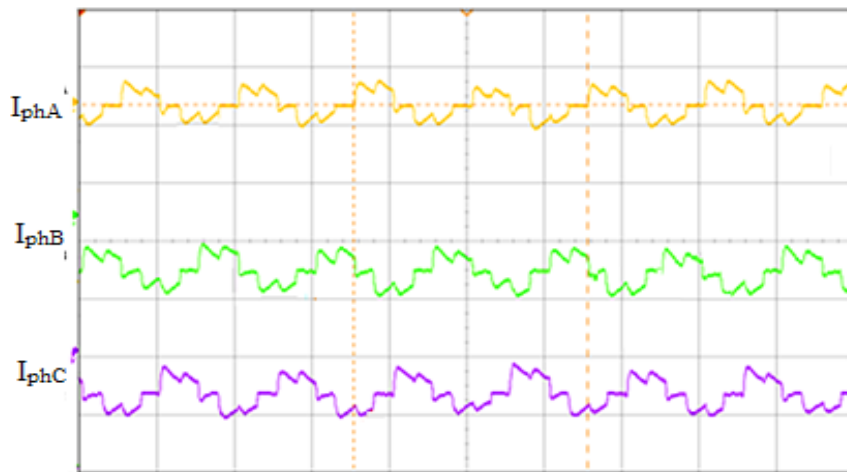


Figure 18. Phase Current in Proposed topology

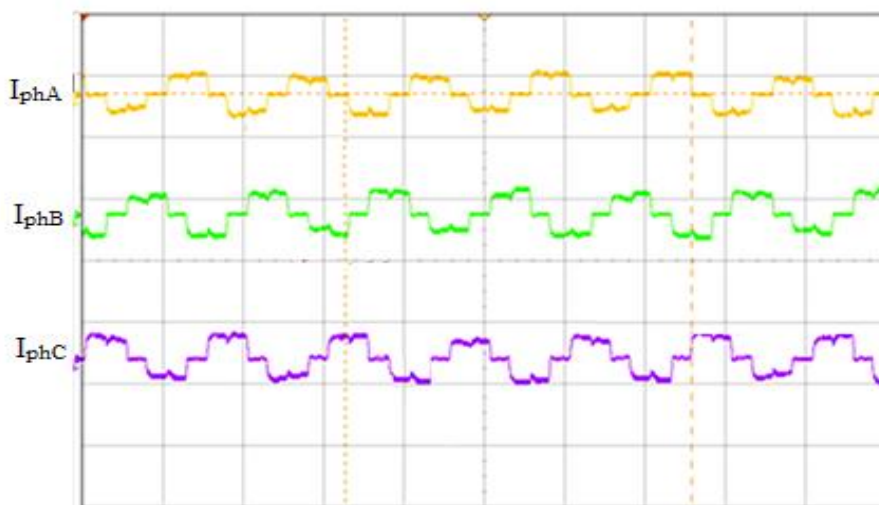


Figure 19. DC link current of the proposed topology

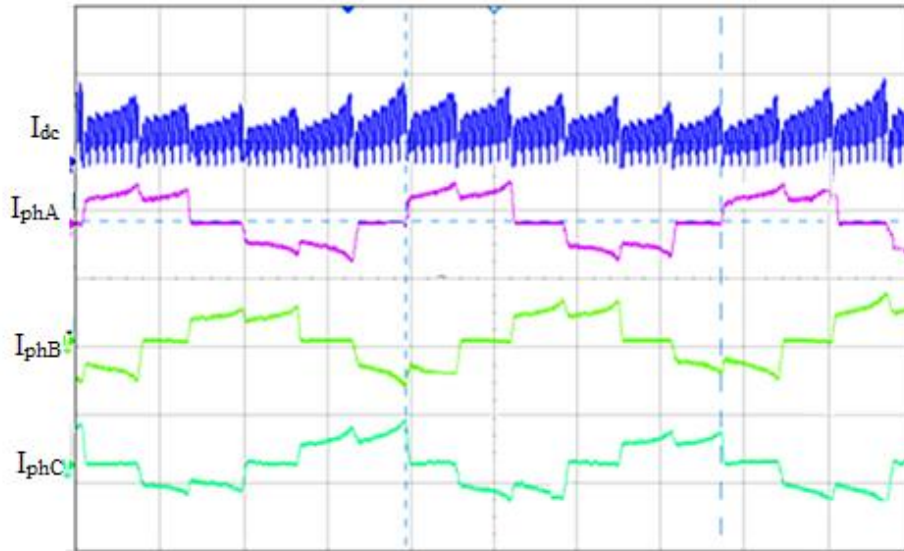
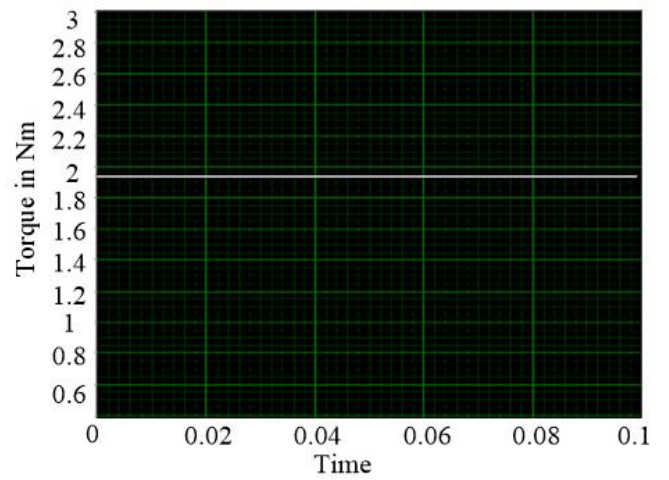
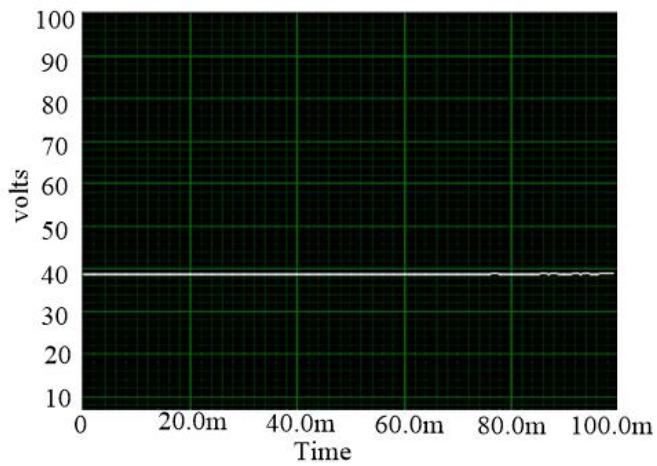


Figure 20(a). Voltage equivalent of torque

Figure 20(b). Experimental result of torque in BLDC motor



List of Tables:

Table 1. Switching pattern of the proposed SVPWM topology

Step/ Mode	Hall Sensor [H _a H _b H _c]			SVPWM Active Vector I _{dc} <I _{th}		Proposed Turned ON/Turned OFF method I _{dc} >I _{th}	
	H _a	H _b	H _c	Active Switches	Active Vector	Case 1	Case 2
1	1	0	0	S ₁ , S ₂	V _{L1} (110000)	V ₀ (100000)	V ₀ (010000)
2	1	1	0	S ₂ , S ₃	V _{L2} (011000)	V ₀ (010000)	V ₀ (001000)
3	0	1	0	S ₃ , S ₄	V _{L3} (001100)	V ₀ (001000)	V ₀ (000100)
4	0	1	1	S ₃ , S ₄	V _{L4} (000110)	V ₀ (000100)	V ₀ (000010)
5	0	0	1	S ₄ , S ₅	V _{L5} (000011)	V ₀ (000010)	V ₀ (000001)
6	1	0	1	S ₅ , S ₆	V _{L6} (100001)	V ₀ (000001)	V ₀ (000001)

Table 2. PMBLDC motor parameters

Parameters	Values
DC input voltage (V)	100
Stator resistance(mΩ)	2.87
Stator Inductance (μH)	850
DC link Capacitance (μF)	200
Maximum threshold current (A)	20
Inertia Constant (Kgm ²)	0.008
Frictional coefficient (Nms)	0.001

Biographies

Indira Damarla is currently working as an Assistant Professor at the Department of Electrical and Electronics Engineering, Velagapudi Ramakrishna Siddhartha Engineering College, Siddhartha Academy of Higher Education Deemed to be University, Vijayawada, India. She completed her bachelor's degree in EEE from Jawaharlal Nehru Technological University, Hyderabad, India in 2005 and her master's degree in Power Electronics and Industrial Drives from Sathyabama University, Chennai, India in 2011. She obtained her PhD degree from Anna University in the area of Switched reluctance motor drives for EV applications. She has twelve years of teaching and four years of research experience. She has a credit of publishing papers in an international conference and in journals. Her research interests are DC-DC power converters, switched reluctance motor drives, renewable energy interfacing, and electric vehicles.

Venmathi Mahendran is an Associate Professor in St. Joseph's College of Engineering, Chennai, Tamil Nadu, India. She obtained her BE from Madras University, Chennai, India in 2003, ME in Power Systems Engineering from College of Engineering, Guindy, Anna University, Chennai, India in 2007. She obtained her PhD degree from Anna University in the area of solar PV systems interfacing converters. She has been working in the teaching field for about 18 years. She has published many papers in conference and journals. Her areas of interest include solar PV systems, power conversion techniques for renewable energy sources.

V. Krishnakumar received the B.E. degree in electrical and electronics engineering from the IFET Engineering College, Gangarampalaiyam, India, in 2007, the M.Tech. degree from the Pondicherry Engineering College, Pillaichavadi, India, in 2010, and the Ph.D. degree from Anna University, Chennai, India, in 2017. He was an Assistant Professor with the Mailam Engineering College, Mailam, from 2010 to 2017. He is currently an Associate Professor with the St. Joseph's College of Engineering, Chennai. His current research interests are improved performance permanent magnet brush-less dc motor drives and performance enhancement of solid-state converters through innovative pulse width modulation strategies.

P. Anbarasan received the B.Tech. degree from Pondicherry University, Kalapet, India, in 2004, the M.Tech. degree from the Pondicherry Engineering College, Pillaichavadi, India, in 2007, and the Ph.D. degree in electrical engineering from Anna University, Chennai, India, in 2019. He has 18 years of teaching and six years of research experience. He is currently an Assistant Professor with the St. Joseph's College of Engineering, Chennai. He has published in journals and conferences in the areas of multilevel inverters and wind energy conversion systems. He also published three Indian patents and granted one Australian innovation patent. His areas of research include dc–dc converters, multilevel inverter topology design, and its application in renewable energy sources.